Journal of Bio- and Tribo-Corrosion (2019) 5:29
https://doi.org/10.1007/s40735-019-0220-1

Characterization and Corrosion Studies of TiAlN PVD Coating by Using the Polarization Test Method

Vijayasarathi Prabakaran[1]

Received: 21 July 2018 / Revised: 20 December 2018 / Accepted: 9 January 2019 / Published online: 23 January 2019

Abstract
In the present study, the TiAlN coatings were deposited on Martensitic stainless steel AISI410 using PVD sputtering technique. In this investigation, the adhesion strength, microstructure, mechanical properties were studied via X-ray diffraction (XRD), non-indentation, and micro-scratch tests. The effect of TiAlN coating on scratch test was also examined by Scanning electron microscope (SEM). Also, a corrosion resistance of the substrate and TiAlN-coated specimen in 3.5% NaCl was evaluated by potentiodynamic polarization method. It was observed that the TiAlN coating exposes superior corrosion resistance than uncoated AISI410 specimen.

Keywords TiAlN coating · Corrosion resistance · SEM-EDX · Surface morphology

1 Introduction

A high alloy stainless steel is used in various applications like gas turbines, engine cam, piston rings, engine inlet value, shafts, heat exchangers in petrochemical industry, impeller, bolts, screws, bushings, nuts, and nozzles [1]. In later years, corrosion behavior of nanostructured materials or coatings is an important topic in corrosion field. Corrosion of iron or steel and high alloy steel is affected by the environment to which these are exposed [2]. Recent surveys indicate that 80% of the full price for the protection of metals is related to coating application. The PVD (physical vapor deposition) methods are usually used nowadays for development of the corrosion, mechanical, and other properties, of a broad range of engineering materials [3–5]. Many recent reports have shown the development made for cutting and drilling lifetime vs speed show, wear and friction reduction, and corrosion resistance when these materials are used in the PVD coating of the tools [6]. Equally, one of the major milestones in the advances of hard coating development, TiN coating was produced in the early 1970s [7] and this hard coating has played a vital role in surface engineering parts for two decades because of high hardness over 20GPa [8]. Transition metal nitride-based hard coatings (especially TiN) have been effectively used for the materials cover since the commercialization of PVD TiN coatings in early 1980s [9–14]. Kalss et al. [15], the beginning of the production of the coatings to be used in cutting applications, TiN films were chosen due to their good mechanical properties. However, the loss of hardness and oxidation of these coatings, at cutting temperatures, refrained the cutting speed. The main part of Al in TiAlN coatings overcomes the oxidation problems due to the comportment of a superficial layer of Al_2O_3 formed at high temperatures [15–23]. In comparison with TiN-based coatings (e.g., TiAlN), CrAlN coatings have been reported to exhibit higher oxidation resistance, as both the chromium and aluminum could form defensive oxides which repressed oxygen dispersion TiAlN thin films are now commercially obtainable as wear-resistant coatings for high-speed machining, due to their high hardness, excellent oxidation, and corrosion resistance [16, 24–32]. The present work aim has been focused to compare the corrosion behavior of TiAlN PVD coating deposited on martensitic stainless steel AISI410 using the Polarization Test method.

✉ Vijayasarathi Prabakaran
vijayasarathisiddhan@gmail.com

[1] Mechanical Engineering, Chalapathi Institute of Engineering and Technology, Chalapathi Nagar, Lam, Guntur, AP 522034, India

2 Experimental Details

The Martensitic stainless steel AISI 410 (composition P 1.0%, Mn 1.0%, C 0.15%, Cr 13.5% S 0.03% Si 1.0%) is used as the substrate material. The specimen with a dimension of 24 mm Ø × 12 mm thick was milled from the stainless steel AISI410 and maintained the surface roughness between 0 and 0.67 µm by conservative machining processes such as turning, facing, and grinding. Prior to surface coating, the steel surface was cleaned using trichloroethylene solvent. After degreasing the specimen, surface was free of grease, oil, and oxide scales, which would then have a harmful effect on the bond of the coating. The TiAlN PVD coating with a thickness around 3.06 ± 1 µm was sputtering on the AISI410 steel surface. After PVD coating, the physical appearance of the TiAlN coating, coating color, uniformity, and the occurrences of any gross defects were inspected visually. The microstructure of the TiAlN-coated surface was evaluated by an optical microscope. The surface structure of the TiAlN-coated surface and grain size of the thin coated surface were measured by scanning electron microscopy and scherrer formula [33] from XRD diffractogram. The corrosion resistance of TiAlN-coated and uncoated AISI410 steel in 3.5% NaCl was assessed by potentiodynamic polarization studies, using a potentiostat/galvanostat/frequency response analyzer of ACM Tools. The three electrodes are working electrode as a TiAlN and uncoated AISI410 steel, while a saturated calomel electrode and a graphite rod helped as the reference and auxiliary electrodes. These three working electrodes were exposed to the 3.5% NaCl only a part of 1 cm^2. The potentiodynamic polarization evaluated was carried out from OCP at a scan rate of 10 mV/min with a potential range from − 250 mV versus SCE in the cathodic direction to + 250 mV versus SCE in the anodic direction. The Tafel extrapolation method was used to estimate the corrosion potential (E_{corr}) and corrosion current density (i_{corr}).

3 Results and Discussions

3.1 Coating Characterization

The optical micrographs of the uncoated and TiAlN-coated substrate are shown in Figure 1. The particle size of the TiAlN coating was evaluated by Scherrer formula from XRD diffractogram. This result shows that the particle size of TiAlN coating was found as 09 nm. Also, the observed TiAlN coatings are uniform and violet gray in color.

3.2 Estimation of Porosity

The TiAlN coatings deposited on a stainless steel material AISI410 by the PVD sputtering method are generally porous in nature while the porosity of coatings deposited by PVD sputtering method depends on the chemical composition of the operating conditions. The porosity of TiAlN coating deposited on AISI410 steel were determined by the following method: A strip of filter paper (20 × 50 mm) was immersed in a solution mixture having 10 g/l potassium ferricyanide, 15 g/l sodium chloride, and 5 g/l gelatin. Subsequently, the filter paper was carefully applied to the coated AISI410 steel sample for 1 min. During this period, the ferrous ions from the uncoated spaces of the AISI410 steel sample would have reacted with ferricyanide existing in the filter paper, resulting in the development of Prussian blue color complex in the filter paper. Hence, a measure of the number of blue spots (Prussian blue color) developed in

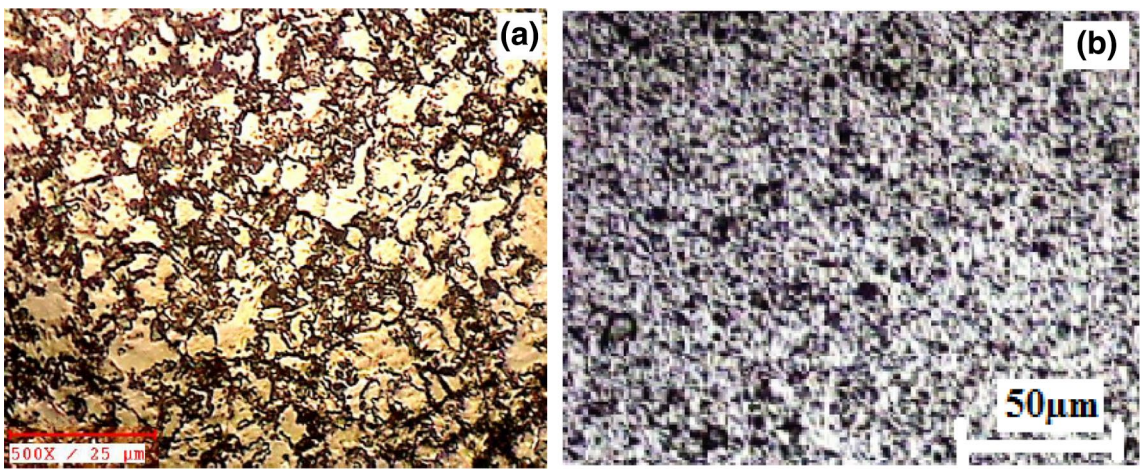

Fig. 1 Optical micrographs of the surface **a** uncoated and **b** TiAlN-coated surface

the filter paper strip per unit area could provide an estimate of the porosity of coatings. This examination is effective in identifying the uniformity of the coating and in locating the occurrence of any gross defects such as bare patches [34–36].

3.3 Progressive Load Scratch Test

The Scratch test was performed on TiAlN coating with a load range of 1N to 150N. It is observed that the critical load LC_3 describes the vital role of coating adhesive strength. Figure 2 shows that the three different systems were identified on TiAlN Coating scratch test, at the base of the acoustic emission (AE) and tangential force (Ft) measured as a function of normal load (Fn). The test result of critical load LC_3 describes that the beginning of the coating peeling was observed by optical microscope as exposed in Figure. 3. Furthermore, the critical load of LC5 describes that the full supremacy of the TiAlN coating on AISI410 steel was observed by optical microscope and frictional force. According to the test result, the average adhesive strength (LC_3) and total delamination (LC_5) of the TiAlN coating are 24N and 79N.

3.4 Surface Morphology

Figure 4a shows the surface morphology of the TiAlN coatings deposited on AISI410 steel substrate using PVD technique. It is noted that the TiAlN coatings have uniform microstructure all over the AISI410 steel surface. The TiAlN coating contains some pores and inclusions as observed in the microstructure. The porosity of the TiAlN coating is 0.4%. The cross section of the TiAlN coatings with a thickness is 3.06 µm ± 1 as shown in Fig. 4b. The particle size of the TiAlN coating

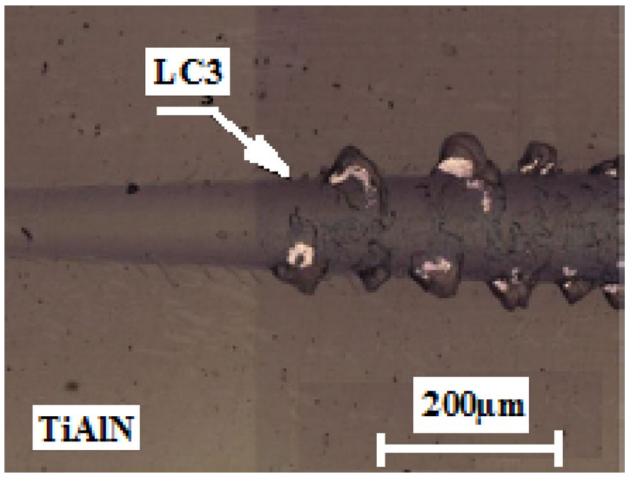

Fig. 3 Optical Images revealing the surface damage during PLST at 1 to 150N

was evaluated by Scherrer formula [33] (Eq. 1) from XRD diffractogram as shown in Figure 5. The particle size of the TiAlN coating is 15 nm which proves higher hardness than the uncoated AISI410 steel. Figure 6 shows the SEM micrograph along with EDS analysis of uncoated and TiAlN-coated AISI410 steel. The EDS analysis is evidence which shows the presence of Ti (62.2%) as the main along with Al (33.85%) and N (3.94%). In addition, the case of uncoated AISI410 steel shows the presence of Fe (74.91%), C (11.92%), Cr (8.83%), O (3.16%), and Si (1.18%).

$$D = 0.9\lambda/B\cos\theta, \tag{1}$$

where D is the grain size of the coated samples, λ is the X-ray wavelength, and B is the full-width at half maximum of a Bragg peak.

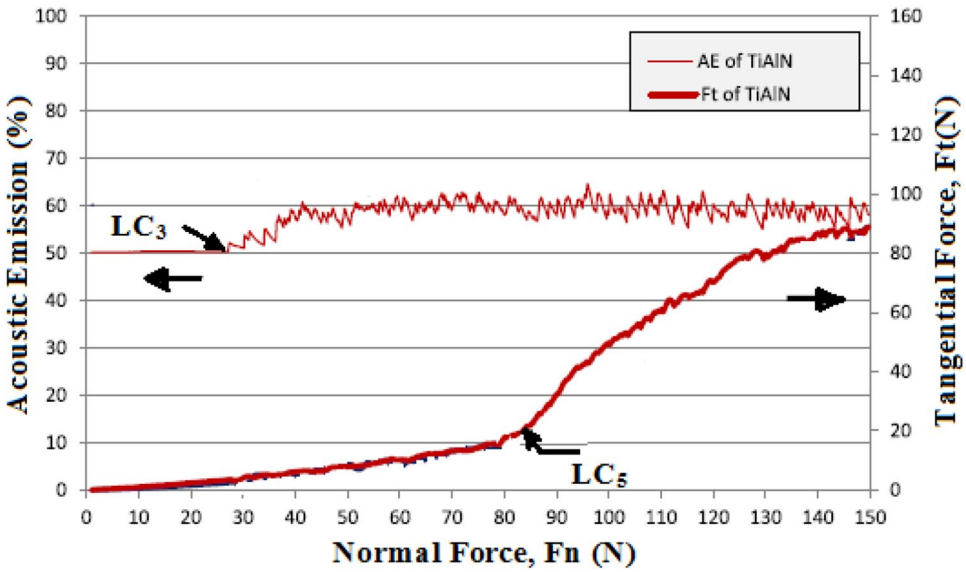

Fig. 2 Plot of the friction coefficient and acoustic emission signal vs Normal Load

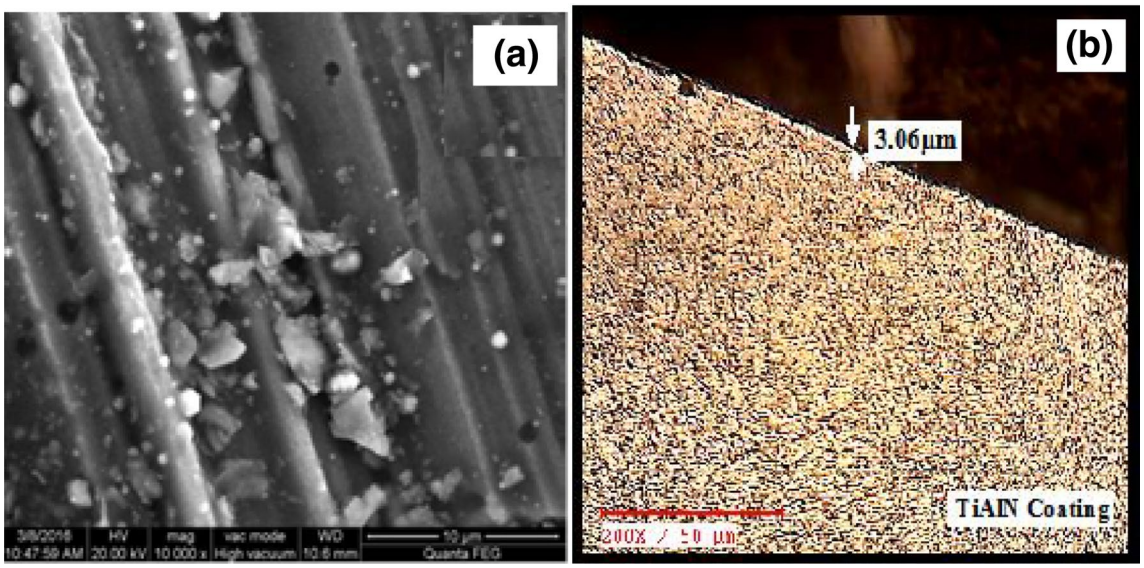

Fig. 4 **a** Surface morphology and **b** Cross section of TiAlN coating

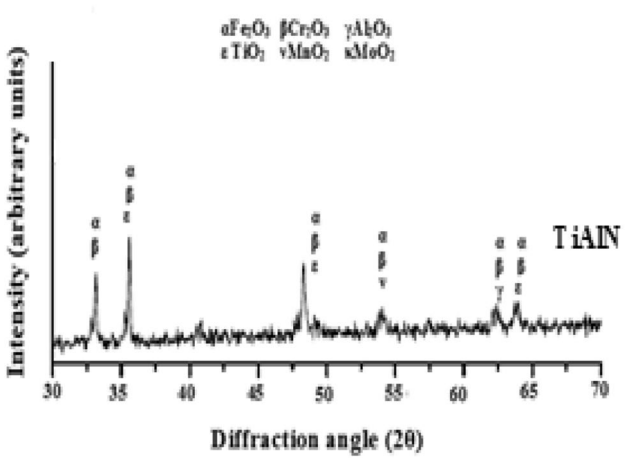

Fig. 5 X-ray diffraction pattern for TiAlN-coated surface illustrated

3.5 Corrosion Behavior of TiAlN Coating Deposited by PVD Method

The potentiodynamic polarization curves of the uncoated AISI410 steel and TiAlN-coated AISI410 steel are shown in Figure 7. The corrosion density and corrosion potential values for uncoated and TiAlN-coated AISI410 steel are shown in Table 1. The intersection of the extrapolation of anodic and cathodic Tafel curves is used to evaluate the corrosion current density and the corrosion potential values. The TiAlN coating has performed best corrosion resistance when compared with uncoated substrate. The test result of the protective efficiency, Pi (%) of the films can be calculated by Eq. (2). The TiAlN coating shows highest protective efficiency of 34.15% because of low current density by 3.5% NaCl solution at room temperature [9].

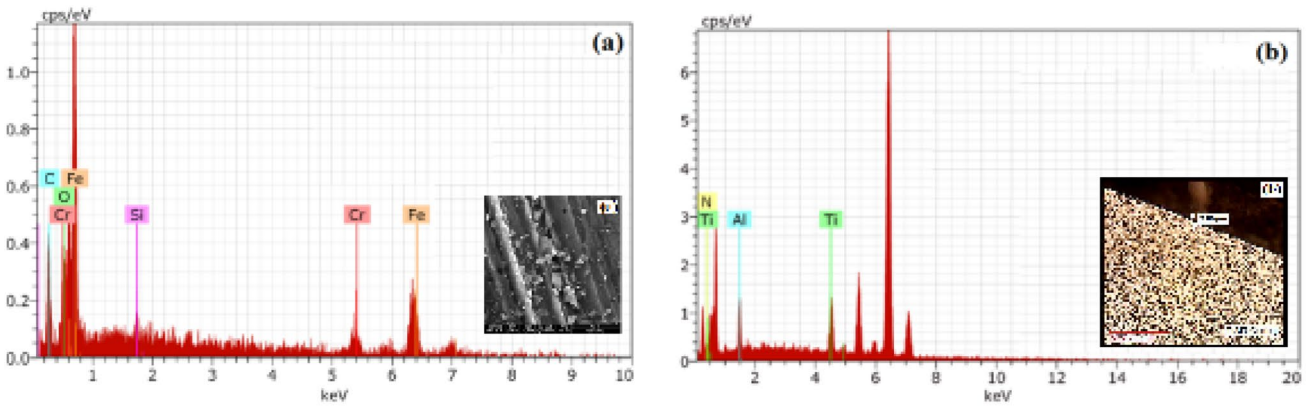

Fig. 6 Energy dispersive X-ray analysis of **a** uncoated steel and **b** TiAlN-coated steel

$$\text{Pi}\ (\%) = \left[1 - \left[\frac{i_{\text{corr}}}{i^0_{\text{corr}}}\right]\right] \times 100 \quad (2)$$

where i_{corr} and i^0_{corr} are the corrosion current density [9].

Further, the corrosion rate (i_{corr}) of the specimens was obtained using the Stern-Geary [2] Eq. (3).

$$i_{\text{corr}} = \frac{1}{2.303} \times \frac{\beta a \beta c}{\text{Rp} \times (\beta a + \beta c)} = \frac{Z}{\text{Rp}}, \quad (3)$$

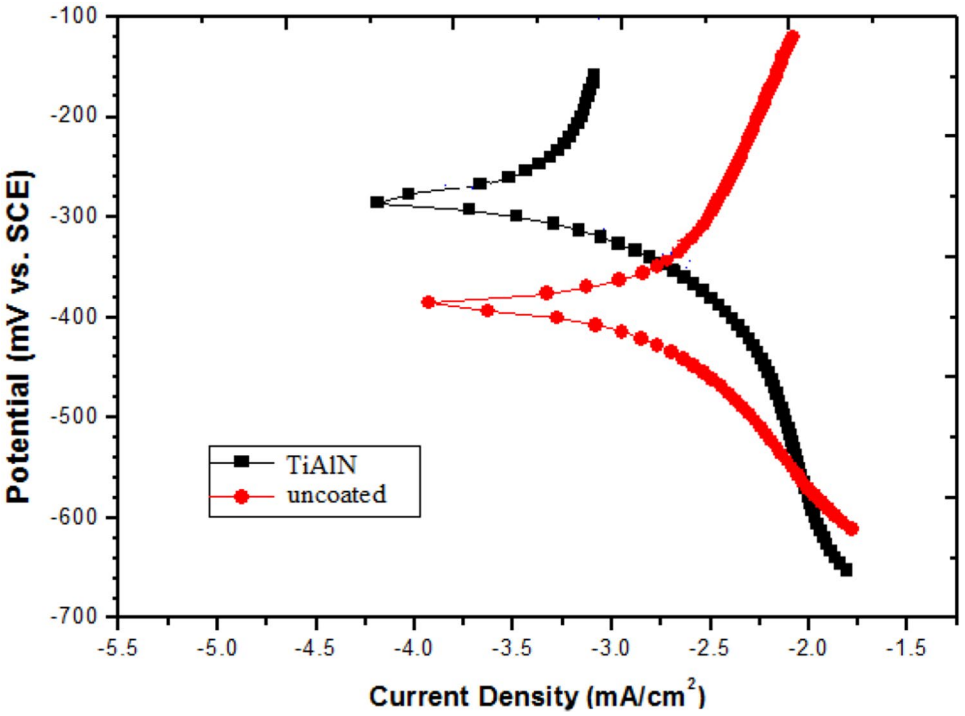

Fig. 7 Potentiodynamic polarization curves of uncoated and TiAlN-coated steel in 3.5% NaCl solution

Table 1 Corrosion potential (E_{corr}), corrosion current density (i_{corr}) and corrosion rate of uncoated and TiAlN composite-coated steel in 3.5% NaCl solution

S. No.	Sample specification	E_{corr} (mV vs SCE)	i_{corr} (μA/cm^2)	Corrosion rate (mils/year)
1	Uncoated	− 392.07	0.001935	1.7956
2	TiAlN	− 285.12	0.001086	0.3923

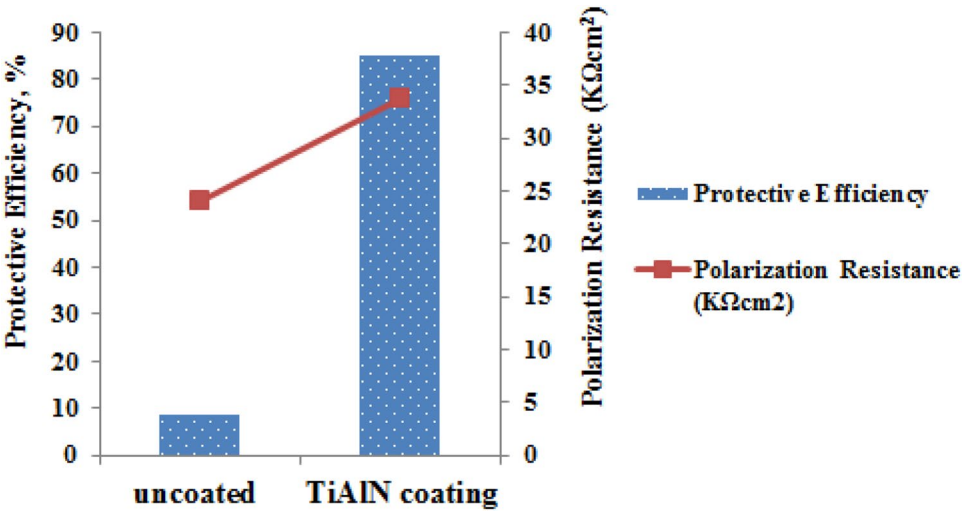

Fig. 8 Protective efficiency and Polarization resistance of uncoated and TiAlN-coated steel

where βa is anodic Tafel slope, βc is cathodic Tafel slope, Rp is polarization resistance, and Z is a function of the Tafel slopes.

The porosity value is obtained from Eq. (4) and the test value is shown in Figure 8.

$$F(\%) = \left[\frac{\text{Rpm}}{\text{Rp}} \times 10^{-\left[\frac{\Delta E_{corr}}{\beta a}\right]}\right] \times 100, \quad (4)$$

where ΔE_{corr} is the corrosion potential variance between the uncoated and TiAlN-coated substrate, Rp is the polarization resistance of the TiAlN-coated substrate, βa is the anodic Tafel constant of the specimen, Rpm is the polarization resistance of the specimen, and F represents porosity. From this analysis, due to the higher porosity of uncoated specimen, the corrosion current density is quite higher than TiAlN coating as shown in Table 1.

4 Conclusion

- The SEM analysis confirms that the surface structure of the TiAlN coating is uniform.
- The XRD and SEM with EDS analysis confirm the composition of coatings.
- The scratch test result confirms the Adhesive strength and total domination of the TiAlN coating are 24N and 79N.
- The TiAlN coating shows highest protective efficiency of 34.15% because of low current density by 3.5% NaCl solution at room temperature
- The TiAlN coating performs very well and showed better corrosion resistance than the uncoated AISI410 steel as evident from corrosion current density and polarization resistance.

Acknowledgements The author would like to thank Sri Y. V. Anjaneyulu, Chairman, Er. D. Vinaykumar, B.Tech, Director, Dr. P. Pandarinath, M.Tech, Ph.D, Principal and Prof N. SatyaNarayana, Senior Professor, Mechanical Department of Chalapathi Institute of Engineering & Technology, Chalapathi Nagar, Lam, Guntur-522034 for their constant encouragement in all endeavors. The author would also like to thank to the reviewer for providing their useful comments, suggestions, and guidelines during the course of revision to improve the technical quality of the present paper.

References

1. Liu L, Li Y, Wang F (2007) Influence of nanocrystallization on passive behavior of Ni-based superalloy in acidic solutions. Electrochim Acta 52:2392–2400
2. Sahoo G, Balasubramaniam R (2008) On the corrosion behaviour of phosphoric irons in simulated concrete pore solution. Corros Sci 50(1):131–143
3. Dobrzanski LA, Lukaszkowiez K, Zarychta V, Cunha L (2005) Corrosion resistance of multilayer coatings deposited by PVD techniques onto the brass substrate. J Mater Process Technol 164–165:816–821
4. Fedrizzi L, Rossi S, Cristel R, Bonora PL (2004) Corrosion and wear behaviour of HVOF cermet coatings used to replace hard chromium. Elect Chem Acta 49:2803–2814
5. Dearnley PA (2017) Introduction to surface engineering. Cambridge University Press, Cambridge
6. Baumvol IJR (1994) New trends in hard coatings technology. Nucl Instr Methods Phys Res B 85:230–235
7. Schintlmeister W, Pacher O (1975) Preparation and properties of hard-material layers for metal machining and jewelry. J Vac Sci Technol 12:743
8. Yoo YH, Le DP, Kim JG, Kim SK, Vinh PV (2008) Corrosion behavior of TiN, TiAlN, TiAlSiN thin films deposited on tool steel in the 3.5 wt.% NaCl solution. Thin Solid Films (516):3544–3548
9. Ding XZ, Tan ALK, Zeng XT, Wang C, Yue T, Sun CQ (2008) Corrosion resistance of CrAlN and TiAlN coatings deposited by lateral rotating cathode arc. Thin Solid Films 516:5716–5720
10. Vijayasarathi P, Kavitha C (2015) An overview of corrosion performance of automotive metals in biodiesel. Res J Eng Technol 6(4):457
11. Vijayasarathi P, Kavitha C (2016) Characterisation and corrosion resistance of TiCrN composite coating on steel by physical vapour deposition method. J Bio Tribo Corrosion 2(4):25
12. Vijayasarathi P (2018) Wear mechanism and tool performanceof TiAlN coated during machining of AISI410 steel. J Bio Tribo Corrosion 4(4):65. https://doi.org/10.1007/s40735-018-01881
13. Vijayasarathi P, Ilaiyavel S, Sureshprabhu P (2017) Evaluation of sliding wear resistance of physical vapor deposited coatings by the ball-cratering test method. J Eng Mater Technol 139(3):031009
14. Vijayasarathi P, Sureshprabhu P et al (2015) Tribological studies of Ti–Al–N hard-faced coatings evaluated with ball-cratering test method. J Chin Soc Mech Eng 36(6):567–573
15. Kalss W, Reiter A, Derflinger V, Gey C, Endrino JL (2006) Modern coatings in high performance cutting applications. Int J Refract Metals Hard Mater 24:399–404
16. Fox-Rabinovich GS, Beake BD, Endrino JL, Veldhuis SC, Parkinson R, Shuster LS, Migronov MS (2006) Effect of mechanical properties measured at room and elevated temperatures on wear resistance of cutting tools with TiAlN and AlCrN coatings. Surf Coat Technol 200:5738–5742
17. Pinkas M, Pelleg J, Daniel MP (1999) Structural analysis of (Ti1–xAlx) N graded coatings deposited by reactive magnetron sputtering. Thin Solid Films 355–356:380–384
18. Suzuki T, Huang D, Ikuhara Y (1998) Microstructures and grain boundaries of (Ti, Al) N films. Surf Coat Technol 107:41–47
19. Zhou M, Makino Y, Nose M, Nogi K (1999) Phase transition and properties of Ti–Al–N thin films prepared by rf-plasma assisted magnetron sputtering. Thin Solid Films 339:203–208
20. Bouzakis KD, Vidakis N, Michailidis N, Leyendecker T, Erkuens G, Fuss G (1999) Quantification of properties modification and cutting performance of (Ti1–xAlx) N coatings at elevated temperatures. Surf Coat Technol 120:34–43
21. von Richthofen A, Cremer R, Witthaut M, Domnick R, Neuschütz D (1998) Composition, binding states, structure, and morphology of the corrosion layer of an oxidized Ti0. 46Al0. 54N film. Thin Solid Films 312:190–194
22. Cunha L, Andritschky M, Rebouta L, Silva R (1998) Corrosion of TiN,(TiAl) N and CrN hard coatings produced by magnetron sputtering. Thin Solid Films 317:351–355
23. Jiménez C, Sanchéz-Fernández C, Morant C, Mart´ınez-Duart JM, Fernández M, Sánchez-Ol´ıas J (1999) Dependence of the mechanical and structural properties of (Ti, Al) N films on the nitrogen content. J Mater Res 14(7):2830–2837
24. Jehn AJ, Baumgartner ME (1992) Corrosion studies with hard coating-substrate systems. Surf Coat Technol 54–55:108

25. Spain E, Avelar-Batista JC, Letch M, Houdsen J, Lerga B (2005) Characterization and application of Cr-Al-N coatings. Surf Coat Technol 200:1507–1513
26. Lin J, Mishra B, Moore JJ, Sproul WD (2008) A study of the oxidation behavior Of CrN and CrAlN thin films in air using DSC and TGA analyses. Surf Coat Technol 202:3272–3283
27. Endrino JL, Fox-Rabinovich GS, Reiter A, Veldhuis SV, Escobar Galindo R, Albella JM, Marco JF (2006) Oxidation tuning in AlCrN coatings. Surf Coat Technol 201:4505–4511
28. Bobzin K, Lugscheider E, Nickel R, Bagcivan N, Krämer A (2007) Wear behavior of Cr1-xAlxN PVD-coatings in dry running condition. Wear 263:1274–1280
29. Kawate M, Hashimoto AK, Suzuki T (2003) Oxidation resistance of Cr1-xAlxN and Ti1-xAlxN films. Surf Coat Technol 165:163–167
30. Benlatreche Y, Nouveau C, Marchal R, Ferreira Martins JP, Aknouche H (2009) Applications of CrAlN trenary system in wood of medium density fiber board (MDF). Wear 267:1056–1061
31. Wang L, Zhong S, Chen Z, Li J, Li M (2012) Influence of deposition parameters on hard Cr-Al-N coatings deposited by multi-arc ion plating. Appl Surf Sci 258:3629–3636
32. Chawla V (2013) Structural characterization and corrosion behavior of nanostructured TiAlN and AlCrN thin coatings in 3 wt% nacl solution. J Mater Sci Eng A 3(1A):22
33. Chawla V, Jayaganthan R, Chandra R (2008) Structural characterizations of magnetron sputtered nanocrystalline TiN thin films. Mater Characterization 59:1015–1020
34. Rausch W (1990) The phosphating of metals. ASM International Materials Park, Ohio and Finishing Publications Ltd., London
35. Rajagopal C, Vasu KI (2000) Conversion coatings—a Reference for phosphating, chromating and anodizing. Tata McGraw-Hill publishing company Ltd., New Delhi
36. Sankara Narayanan TSN (2005) Surface pretreatment by phosphate conversion coatings—a review. Rev Adv Mater Sci 9:130–177